

Article

# Assessing the Difference in the Climate Elasticity of Runoff across the Poyang Lake Basin, China

Hongxiang Fan <sup>1,2</sup>, Ligang Xu <sup>1,\*</sup>, Hui Tao <sup>1</sup>, Wenjuan Feng <sup>1,2</sup>, Junxiang Cheng <sup>1,2</sup> and Hailin You <sup>3</sup>

<sup>1</sup> Key Laboratory of Watershed Geographic Sciences, Nanjing Institute of Geography and Limnology, Chinese Academy of Sciences, Nanjing 210008, China; fanhongxiang13@mails.ucas.ac.cn (H.F.); htao@niglas.ac.cn (H.T.); fengwenjuan16@126.com (W.F.); junxiang1118@163.com (J.C.)

<sup>2</sup> University of Chinese Academy of Sciences, Beijing 100049, China

<sup>3</sup> Poyang Lake Research Center, Jiangxi Academy of Sciences, Nanchang 330096, China; youhailin1985@163.com

\* Correspondence: lgxu@niglas.ac.cn; Tel.: +86-153-6605-1586

Academic Editor: Athanasios Loukas

Received: 30 August 2016; Accepted: 11 February 2017; Published: 20 February 2017

**Abstract:** Understanding the effects of climate and catchment properties' changes on water yield is a challenging component in assessments of future water resources. Here, we spatially applied the water-energy balance equation, based on the widely-used Budyko framework, to quantify the temporal and spatial differences of the climate elasticity of runoff in the Poyang Lake Basin (PYLB), highlighting the influence of the catchment properties' parameter  $n$  variation on the climate elasticity and runoff prediction. By using Sen's slope and the Mann–Kendall method, we found that, for the whole study period (1960–2010), annual temperature in PYLB significantly increased at a rate of 1.44% per decade. Basin-wide wind speed and net radiation had been declining at 0.17 m/s and 46.30 MJ/m<sup>2</sup> per decade. No significant trend was detected in precipitation and relative humidity. The moving average method was applied to evaluate the temporal pattern of  $n$ . The results showed that the calibrated catchment properties' parameter and the derived elasticities were not constant during the past 50 years. We found that in most sub-basins, the  $n$  values increased during 1970–1980, followed by a decreasing trend in the period from 1980 to 1990, whereas the  $n$  value in Fuhe sub-basin kept increasing for the almost the whole study period. In addition, the climate elasticity is highly correlated with the  $n$  value, indicating that the catchment properties' parameter was the dominant factor influencing climate elasticity in PYLB in the past 50 years. We also attempted to predict the runoff trend with the consideration of trends in  $n$ . However, in some sub-basins, there were still considerable differences between the predicted runoff trend and the observed one. The method used here to evaluate the temporal pattern of  $n$  should be an extension of the existing literature and will provide a better understanding of elasticity in the regional hydrological cycle.

**Keywords:** Budyko; runoff; Poyang Lake Basin; elasticity

## 1. Introduction

Recently, the climate has changed considerably [1], and many of the observed changes are unprecedented over decades to millennia [2]. Hence, understanding the change in regional water availability and hydrological cycle under a warming climate is of great importance for sustainable development of human society, ecosystem services, as well as the regional water resources' management [3–6]. Planning for potential future changes in water yield requires not only an understanding of possible climate change, but also understandings of how and to what extent a catchment's hydrology might respond to such change. However, estimations of future climatic conditions are currently poorly suited to hydrological prediction [7], while climate elasticity

is considered as an important indicator for quantifying how the runoff would change in response to climate change [5,8,9]. The climate elasticity was defined by Fu [8] as the proportion of the change in runoff to the change in climate variables. Following that, various methods have been developed to compute the climate elasticity. Sankarasubramanian et al. [6] well classified these methods into five categories: (1) varying the input of a calibrated conceptual watershed model to observe the resulting runoff change; (2) analytically derivation; (3) fitting multivariate regional hydrological models; (4) empirical estimation based on historical data; and (5) applying multivariate statistical methods. The model-based approach might be physically sound, but requires major efforts on model calibration and can lead to remarkably different results because of the uncertainty in model structure and parameter estimation [10–13]. Moreover, given that climatic conditions are not stationary [14], such hindcasting approaches are problematic for prediction. In contrast, the Budyko hypothesis ingeniously couples hydrological cycle and terrestrial energy balance [3,15–17], which contains not only the regional climate conditions, but also the parameter reflecting underlying characteristics [18–22]. Based on the Budyko hypothesis, more generic methods of elasticity have been developed [6,16], amongst which, the analytical derivation approach, depending less on historical data, is clear in theory and, hence, has captured much attention [3,4,9,16,18].

In light of the derivation approach, a unified framework for assessing the elasticity of runoff to changes in average precipitation  $P$  and potential evaporation  $E_0$  has been recently established [3,18,23,24]. This framework renders climate elasticity analyses highly accessible, such that it can be applied wherever long-term average precipitation and other climate data exist. Additionally, the framework can be used to assess different hydrological responses likely across different regions of a catchment or basin, which is important for management decisions relating to possible future hydrological conditions. Consequently, it has been widely applied in many studies to evaluate the impact of climate change on runoff [3,4,18,20,23]. Although the simple framework is powerful for assessing the impacts of average precipitation  $P$  and potential evaporation  $E_0$  on runoff, the variations in potential evaporation are hardly measured due to its inconvenience in calculation, which requires many data [25]. Is it possible to separate the influences of potential evaporation into the influences of more accessible climate variables (e.g., temperature, relative humidity, wind speed, etc.)? Since these climate variables' influences cannot be derived simply based on the water-energy balance equation introduced by previous studies (the M-C-Y equation) [16,26,27], more efforts are needed to figure it out. Yang and Yang [3] recently introduced an analytical solution to this problem by combining the original M-C-Y equation with the Penman equation [28], which made it possible to relate the elasticity of runoff to net radiation, temperature, wind speed and relative humidity, providing a guide for separating the effects of different climate variables on runoff.

Due to its high accessibility, the above-mentioned framework has been widely used. Many previous studies, however, attempted to derive the climate elasticity based on a single (maybe slightly different in forms) Budyko-type curve [5,6,9,23,24]. In accordance with the derived climate elasticity by Yang and Yang [3], we could expect that not only the changes in climate conditions, but also the variation in catchment properties will impact the derived elasticity. To our knowledge, Zheng et al. [23] appears to be the first to demonstrate the temporal variation of climate elasticity using a moving average method, but he did not pay attention to the temporal variation of catchment properties. The inclusion of changes in catchment properties over time seems to have been first considered by Yang et al. [21], but they assumed that the catchment properties would remain constant in that study, and no further calculation of the associated elasticity was made. Following that, Roderick and Farquhar [18] first introduced a qualitative way to explain why the catchment properties would vary over time, but their work also did not consider how the catchment properties' parameter might change over time. Recently, more and more attention has been paid to the variation of catchment properties and its impact on the climate elasticity. As no definitive process-based understanding of what determines the catchment properties' parameter is currently available, it is hard to give an a priori estimate of the parameter [4,29]. Consequently, some studies tried to relate the catchment properties to other climate

factors, such as climate seasonality and mean storm depth [29], while some attempted to link it to vegetation coverage or effective rooting depth and plant root characteristics [20,29]. The key papers related to the Budyko-based framework are summarized in Table 1. As the key factors influencing the catchment properties' parameter remain vague, the evaluation of the climate elasticity variation with the consideration of the change in catchment properties should be an extension of the existing literature and will provide a better understanding of elasticity in the regional hydrological cycle.

**Table 1.** Summary of the relevant literature on the climate elasticity of runoff studies based on the Budyko hypothesis in relation to the aims of the present study. In the second column, the consideration of the catchment properties' parameter is identified by the code: (a) consider the spatial variation of the parameter over different catchments; (b) consider the temporal variation of the parameter. We add the current study for completeness.

Study	Research Focus/Considering Catchment Properties Variation or Not	Data/Length of Time Series/Theory	Location/Catchment(s) Analyzed/Size of the Catchment(s)	Key Results on Catchment Properties
1. Yang et al. [21]	the complementary relationship in non-humid environments/(a)	daily data from 238 meteorological stations/1960–2000/Budyko and Penman hypotheses	China/108 catchments/272–94,800 km <sup>2</sup>	The catchment properties' parameter has a significant regional pattern and represents the land surface conditions.
2. Yang et al. [22]	relate catchment properties parameter to limited landscape characteristics/(a)	daily data from 238 meteorological stations/1951–2000/Budyko hypothesis (Fu's curve)	China/108 catchments/272–94,800 km <sup>2</sup>	The catchment properties' parameter can be estimated from regional characteristics by an empirical formula without calibration
3. Yang et al. [19]	relationships between vegetation coverage and regional water balance/(a)	daily data from 238 meteorological stations/1956–2005/Budyko hypothesis	China/99 catchments/272–46,827 km <sup>2</sup>	The estimation of the inter annual variability of regional water balance can be improved by considering the inter annual variability of vegetation coverage
4. Yang and Yang [3]	climate elasticity of runoff/(a)	daily data from 238 meteorological stations/1951–2000/Budyko curve	China/89 catchments/272–46,827 km <sup>2</sup>	Climate elasticity was sensitive to catchment characteristics
5. Roderick and Farquhar [18]	climate elasticity of runoff/(b)	modeled data [30,31]/1981–2006/Budyko hypothesis	Australia/Murray Darling Basin/1,060,000 km <sup>2</sup>	They gave a qualitative description of why the catchment properties' parameter will change over time
6. Donohue et al. [4]	precipitation and potential evaporation elasticity/(a)	modeled data [30,31]/1981–2006/Budyko hypothesis	Australia/Murray Darling Basin/1,060,000 km <sup>2</sup>	catchment properties' parameter varied over the basins without apparent spatial pattern
7. Donohue et al. [29]	to incorporate key ecohydrological processes into Budyko's hydrological model/(a)	modeled data using BCP model/1981–2006/Budyko hypothesis	Australia/Murray Darling Basin/1,060,000 km <sup>2</sup>	The catchment properties' parameter is closely related to the effects of soil water holding capacity, effective rooting depth and storm depth and could be priori estimated
8. Cong et al. [20]	to understand the hydrological trends in five major basins in China/(b)	daily data from 317 weather stations/1956–2005/Budyko hypothesis	China/5 catchments/315,000–1,781,000 km <sup>2</sup>	The catchment properties' parameter is closely related to effective rooting depth and its trend should be taken into account.
9. This study	climate elasticity/(a) and (b)	daily data from 14 meteorological stations/1960–2010/Budyko hypothesis	China/Poyang Lake Basin (PYLB) /162,225 km <sup>2</sup>	The catchment properties' parameter is the dominant factor influencing climate elasticity in PYLB in the past 50 years.

The Poyang Lake Basin (PYLB) provides a good example where hydrological characteristics vary across space and where management strategies need to be carefully targeted. The objectives of this paper are to (1) evaluate the trend in climatic and hydrologic variables across PYLB during the past 50 years; (2) figure out how the catchment properties' parameter would change over time in PYLB during the past 50 years; (3) determine the spatial and temporal pattern of climate elasticity of runoff across PYLB; and (4) evaluate the impact of catchment properties' parameter variation on the derived elasticities and runoff prediction.

## 2. Study Area and Data Preparation

### 2.1. Overview of the Poyang Lake Basin

Located on the middle and lower reaches of the Yangtze River on the south shore, Poyang Lake (Figure 1) is the largest freshwater lake and an important ecological function protected area in China [32]. The lake has a drainage basin area of 162,225 km<sup>2</sup>, covering about 97% of Jiangxi province [33]. The topography of the Poyang Lake Basin (PYLB) varies from highly mountainous regions (maximum elevation of 2200 m above sea level) to alluvial plains in lower reaches of the primary water resources [34,35]. Poyang Lake exchanges water with the Yangtze River through a narrow outlet located in Hukou [35], while receiving water from the five sub-drainage basins of Ganjiang River, Fuhe River, Xinjiang River, Raohe River and Xiushui River [36,37]. Headwater of these rivers is located in boundaries of the east, south and west of Jiangxi Province that are surrounded by high mountains. The stream gradient decreases as these rivers flow onto the relatively flat region surrounding Poyang Lake. The flat central area of the Poyang Lake Basin is an important region for farming (major crops are rice and oilseed rape) [35], not only in Jiangxi province, but also in China [34]. The PYLB belongs to a subtropical wet climate zone with an annual mean precipitation of 1680 mm and annual mean temperature of 17.5 °C. The hydrological processes in PYLB is complex [36,38], leading to dramatic seasonal water-level fluctuations of Poyang Lake. In normal years, Poyang Lake can expand to a large water surface of 4000 km<sup>2</sup> with a volume of  $3.2 \times 10^{10}$  m<sup>3</sup> and will shrink to little more than a river during the dry season, shaping the unique landscape that has been described as “flooding like the sea, drying like thread” [34,39].

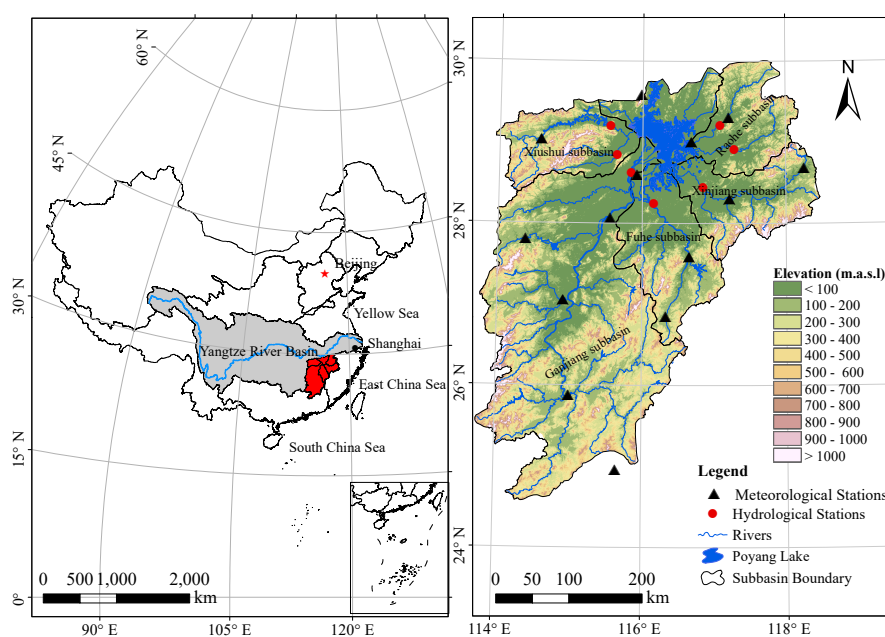


**Figure 1.** Topography and river networks of PYLB. Locations of the 14 meteorological stations and seven hydrological stations are presented using black triangles and red dots, respectively.

### 2.2. Data Preparation

Observed discharges (daily runoff) of seven gauging station (Figure 1) on the lower reaches of the five rivers were obtained from Management Bureau of the Yangtze River (MBYR) catchment for the period from 1960 to 2010. For sub-basins of the Ganjiang, Fuhe and Xinjiang, only one gauging station at each main stream was selected to represent basin runoff, contributing more than 90% of the total inflow of the five rivers; while for sub-basins of the Xiushui and Raohe, gauging stations at tributaries (Wanjiabu station for the Xiushui River, Hushan and Dufengken stations for the Raohe River) were

included to account for the runoff contributions to the main stream, contributing less than 10% of the total inflow of the five rivers. The basic features of these gauging stations are listed in Table 2. The total drainage area of these gauging stations is 137,143 km<sup>2</sup>, leaving an area of 25,082 km<sup>2</sup> (15.5% of the whole basin area, including the lake surface) that is not gauged.

**Table 2.** List of hydrological gauging stations used in this study.

Gauging Station	Location	Coordinates	Gauged Area (km <sup>2</sup> )
Qiujin	Xiushui	115.41° E, 29.10° N	9914
Wanjiabu	Liaohe tributary of Xiushui	115.65° E, 28.85° N	3548
Waizhou	Ganjiang	115.83° E, 28.63° N	80,948
Lijiadu	Fuhe	116.17° E, 28.22° N	15,811
Meigang	Xinjiang	116.82° E, 28.43° N	15,535
Hushan	Le'an tributary of Raohe	117.27° E, 28.92° N	6374
Dufengken	Changjiang tributary of Raohe	117.12° E, 29.16° N	5013

The meteorological data from 14 National Meteorological Observatory (NMO) stations inside the PYLB were obtained from the National Climate Centre of China Meteorological Administration (CMA), including daily observations of air temperature, wind speed, relative humidity, sunshine hours and absolute vapor pressure, among others. The period of records used here is 1960–2010. Based on the meteorological data, potential evapotranspiration (*PET* or *E<sub>0</sub>*) of each weather station was then estimated following the Penman–Monteith method recommended by the Food and Agriculture Organization of the United Nations (FAO), and the computation of all of the data required for the potential evaporation followed the method and procedure given in Chapter 3 of FAO Paper 56 [40].

All of the daily runoff records and climate data provided by MBYR and CMA had gone through a standard quality control process before delivery [34,41,42]. No missing data were found in the variables used in this study, except for daylight hours. The missing daylight hours data were further interpolated using data from the nearest three meteorological stations.

As the Penman–Monteith equation [40] is highly non-linear, consequently, instead of applying the Penman–Monteith equation [40] with basin average variables, we calculated the daily *E<sub>0</sub>* for each weather station using daily hydro-meteorological records. Following that, all of the hydro-meteorological records, as well as the calculated *E<sub>0</sub>* were aggregated from daily to monthly and to yearly. In addition, the large degree of variation in topography and the uneven distribution of weather stations across the PYLB are noticeable and should be taken into consideration when estimating the basin average data. Consequently, Ye et al. [34] suggested that an area-based weighing method (i.e., Thiessen polygon method [43]) should be used in calculating the average data. In the present study, we followed the same procedure used by Ye et al. [34] when calculating the average value of climate variables and potential evapotranspiration for the whole PYLB, as well as the five sub-basins.

### 3. Methodology

#### 3.1. Trend Analysis for Hydro-Meteorological Variables

In the present study, two non-parametric methods (Mann–Kendall test and Sen's slope estimator) were used to detect the trend of climatic variables in PYLB, using temporally- and spatially-aggregated data, namely annual data averaged over five sub-basins.

##### 3.1.1. Mann–Kendall Test

The Mann–Kendall test statistics *S* [44] is calculated as:

$$S = \sum_{i=1}^{n-1} \sum_{j=i+1}^n \text{sgn}(x_j - x_i) \quad (1)$$

where  $n$  is the number of data points.  $x_i$  and  $x_j$  are the data values in times series  $i$  and  $j$  ( $j > i$ ), respectively, and  $\text{sgn}(x_j - x_i)$  is the sign function defined as:

$$\text{sgn}(x_j - x_i) = \begin{cases} +1 & \text{if } x_j - x_i > 0 \\ 0 & \text{if } x_j - x_i = 0 \\ -1 & \text{if } x_j - x_i < 0 \end{cases} \quad (2)$$

The variance is calculated as:

$$\text{Var}(S) = \frac{n(n-1)(2n+5) - \sum_{i=1}^m t_i(t_i-1)(2t_i+5)}{18} \quad (3)$$

where  $n$  is the number of data points,  $m$  is the number of tied groups and  $t_i$  denotes the number of ties of extent  $i$ . A tied group is a set of sample data having the same value. In cases where the sample size  $n > 10$ , the standard normal test statistic  $Z_S$  is computed as follows:

$$Z_S = \begin{cases} \frac{S-1}{\sqrt{\text{Var}(S)}} & \text{if } S > 0 \\ 0 & \text{if } S = 0 \\ \frac{S+1}{\sqrt{\text{Var}(S)}} & \text{if } S < 0 \end{cases} \quad (4)$$

Positive values of  $Z_S$  indicate an increasing trend, while negative  $Z_S$  values mean a decreasing trend. Testing the trend is done at the specific  $\alpha$  significance level. When  $|Z_S| > Z_{1-\alpha/2}$ , the null hypothesis is rejected, and a significant trend exists in the time series.  $Z_{1-\alpha/2}$  can be obtained from the standard normal distribution table. In this study, significance levels  $\alpha = 0.05$  and  $\alpha = 0.01$  were used. At the 5% significance level, the null hypothesis of no trend is rejected if  $|Z_S| > 1.96$  and rejected if  $|Z_S| > 2.56$  at the 1% significance level.

### 3.1.2. Sen’s Slope Estimator

Sen [45] developed the non-parametric procedure for evaluating the slope of trend in the sample of  $N$  pairs of data:

$$Q_i = \left( \frac{x_j - x_k}{j - k} \right) / dt \text{ for } i = 1, \dots, N \quad (5)$$

where  $x_j$  and  $x_k$  are the data values at times  $j$  and  $k$  ( $j > k$ ), respectively.  $dt$  is the desired time interval.

If there is only one datum in each time period, then  $N = \frac{n(n-1)}{2}$ , where  $n$  is the number of time periods. Otherwise,  $N < \frac{n(n-1)}{2}$ , where  $n$  is the total number of observations.

The  $N$  values of  $Q_i$  are sorted from smallest to the largest, and the median of the slope or the Sen’s slope estimator is then computed as:

$$Q_{med} = \begin{cases} Q_{[(N+1)/2]} & \text{if } N \text{ is odd} \\ (Q_{[N/2]} + Q_{[n+2]/2})/2 & \text{if } N \text{ is even} \end{cases} \quad (6)$$

where the sign of  $Q_{med}$  reflect the data trend pattern, while its value indicates the steepness of the trend. Once the slope  $Q_{med}$  has been calculated, the regression line can then been determined from the sample points by setting the intercept  $b$  to be the median of the values of  $y_i - Q_{med} \times x_i$  [46].

### 3.2. Calibration of the Catchment Properties Parameter

Budyko [15] quantified mean annual water balance in terms of the ratio of mean annual evaporation to mean annual precipitation,  $E/P$ , demonstrating that  $E/P$  is determined, to first order, by the ratio of mean annual potential evaporation to mean annual precipitation,  $E_0/P$  (the so-called

climatic dryness index), a measure of climatic aridity. Many attempts have been made to formulate the mean annual water-energy balance. Bagrov [47] first derived the analytical equation for the mean annual water-energy balance by introducing  $dE/dP = 1 - (E/E_0)^n$ . A modification of that formula was derived by Mezentsev [27] and was expressed as  $dE/dP = [1 - (E/E_0)^n]^{(n+1/n)}$ . More efforts have been made for that equation, and it was finally expressed in a generalized form (the M-C-Y equation) [16,26,27]:

$$E = \frac{E_0 P}{(P^n + E_0^n)^{1/n}} \quad (7)$$

where  $E_0$  is the potential evaporation,  $E$  is the actual evaporation  $P$  is the precipitation and  $n$  (dimensionless) is a catchment-related parameter, which modifies the partitioning of  $P$  between  $E$  and  $Q$ .

In terms of Equation (7),  $n$  is the main model parameter that needs to be calibrated. The values of  $n$  are typically in the range of 0.6–3.6, and most are in a smaller range from 1.5 to 2.6 [3,16,18,26]. A default value of  $n$  is recommended by Choudhury [26] as 1.8. In this study, the inhomogeneous characteristics of each sub-basin have been taken into consideration when estimating  $n$ . Apart from the spatial pattern of  $n$ , we also aim to evaluate the temporal variation of  $n$  and its subsequent effects on climate elasticity estimation. In fact, the  $n$  value can be estimated according to Equation (7) whenever the annual mean values of climatic and hydrologic variables are available. Note that the Budyko framework used here assumes steady state conditions and therefore requires a time scale whereby changes in catchment storage are small relative to the magnitude of fluxes (i.e.,  $P, E, R$ ) [4]. In practice, this requires averages over at least one year [18], and previous studies often applied the Budyko framework with averages over 10 years [23,34], 30 years [18] and even longer periods [3]. In the present study, we assume that it would be appropriate to apply the Budyko framework based on the 10-year average. In addition, with that assumption in mind, we further assume that the Budyko framework can be further applied with 10-year moving averages. Following the assumption, the annual values of the related climatic and hydrologic variables were first calculated using the moving average method. The moving window length used in the present study was 10-year. After that, we estimated the parameter  $n$  based on  $\bar{R}$  (mean annual runoff) and  $\bar{P}$  (mean annual precipitation) for each sub-basin within each moving window in order to obtain exact agreement with observations. The calibration was done using a Newton–Raphson method with a desired accuracy of 0.001 [48]. The correlation coefficient and mean absolute error (MAE) between the simulated and observed runoff within each moving window were further calculated to evaluate the calibration results of  $n$  [34].

### 3.3. Derivation of Climate Elasticity

Climate elasticity was derived following the same framework developed by Yang and Yang [3], except for the potential evaporation equation used. As mentioned before, the potential evaporation was estimated following the Penman–Monteith method recommended by FAO [40]. By combining Equation (7), which can be denoted as  $f(E_0, P, n)$ , and the Penman–Monteith equation, which is denoted as  $v(Rn, T, U, RH, \dots)$ , the changes in  $E$  due to changes in climate and the catchment properties can be derived. To first order, the change in  $E$  is:

$$\begin{aligned} dE &= \frac{\partial f}{\partial P} dP + \frac{\partial f}{\partial E_0} dE_0 + \frac{\partial f}{\partial n} dn \\ &\approx \frac{\partial f}{\partial P} dP + \frac{\partial f}{\partial E_0} \frac{\partial v}{\partial Rn} dRn + \frac{\partial f}{\partial E_0} \frac{\partial v}{\partial T} dT + \frac{\partial f}{\partial E_0} \frac{\partial v}{\partial U} dU + \frac{\partial f}{\partial E_0} \frac{\partial v}{\partial RH} dRH + \frac{\partial f}{\partial n} dn \end{aligned} \quad (8)$$

When evaluating the trend in annual evaporation or runoff for a long period (10 years in this study), the water balance equation can be simplified as  $R = P - E$ , which leads to the differential form  $dR = dP - dE$ . By direct substitution into Equation (8), we obtain:

$$dR \approx \left(1 - \frac{\partial f}{\partial P}\right)dP - \frac{\partial f}{\partial E_0} \frac{\partial v}{\partial Rn} dRn - \frac{\partial f}{\partial E_0} \frac{\partial v}{\partial T} dT - \frac{\partial f}{\partial E_0} \frac{\partial v}{\partial U} dU - \frac{\partial f}{\partial E_0} \frac{\partial v}{\partial RH} dRH - \frac{\partial f}{\partial n} dn \quad (9)$$

and the relative change in  $R$  is:

$$\begin{aligned} \frac{dR}{R} &\approx \left[\frac{P}{R} \left(1 - \frac{\partial f}{\partial P}\right)\right] \frac{dP}{P} - \left[\frac{Rn}{R} \frac{\partial f}{\partial E_0} \frac{\partial v}{\partial Rn}\right] \frac{dRn}{Rn} - \left[\frac{T}{R} \frac{\partial f}{\partial E_0} \frac{\partial v}{\partial T}\right] \frac{dT}{T} \\ &- \left[\frac{U}{R} \frac{\partial f}{\partial E_0} \frac{\partial v}{\partial U}\right] \frac{dU}{U} - \left[\frac{RH}{R} \frac{\partial f}{\partial E_0} \frac{\partial v}{\partial RH}\right] \frac{dRH}{RH} - \left[\frac{n}{R} \frac{\partial f}{\partial n}\right] \frac{dn}{n} \\ &= \epsilon_P \frac{dP}{P} + \epsilon_{Rn} \frac{dRn}{Rn} + \epsilon_T \frac{dT}{T} + \epsilon_U \frac{dU}{U} + \epsilon_{RH} \frac{dRH}{RH} + \epsilon_n \frac{dn}{n} \end{aligned} \quad (10)$$

The terms in square brackets can be called the sensitivity coefficients and are analytical expressions formally equivalent to the “elasticity” concept [3,18,49]. The calculation was done using the R statistical software 3.3.2 [50].

#### 3.4. Runoff Prediction with Climate Elasticity

By combining the trend results (Section 3.1) and the derived elasticities, the predicted trend in runoff can be calculated. As mentioned before, most previous studies often predict the runoff trend using climate elasticities with no consideration of changes in catchment properties. In other words,  $dn$  is treated as zero, and the trend in runoff can be denoted as:

$$\frac{dR}{R} = \epsilon_P \frac{dP}{P} + \epsilon_{Rn} \frac{dRn}{Rn} + \epsilon_T \frac{dT}{T} + \epsilon_U \frac{dU}{U} + \epsilon_{RH} \frac{dRH}{RH} \quad (11)$$

However, it is problematic if the temporal variation in  $n$  cannot be neglected. Hence, in addition to Equation (11), we also predicted the runoff trend with consideration of  $n$  variation using Equation (10). Following that, the absolute differences between the two predicted runoff trends, namely trends from Equations (10) and (11), and the observed trend (Section 3.1) were calculated to evaluate the influence of  $n$  on runoff prediction.

## 4. Results

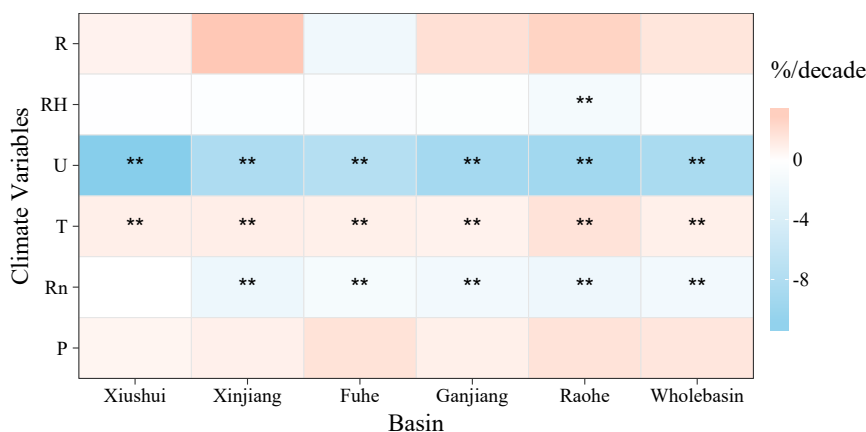
### 4.1. Trend in Climatic and Hydrologic Variables

Following Section 2.2, the average values of the climatic and hydrologic variables across the PYLB were calculated. The results are listed in Table 3. As shown in Table 3, the mean annual precipitation  $\bar{P}$  is 1575.7 mm·year<sup>-1</sup>, 1810.2 mm·year<sup>-1</sup>, 1670.8 mm·year<sup>-1</sup>, 1558.7 mm·year<sup>-1</sup> and 1729.6 mm·year<sup>-1</sup> for Xiushui, Xinjiang, Fuhe, Ganjiang and Raohe, respectively. The maximum value of  $\bar{R}$  is in Xinjiang sub-basin, with a value of 1151.8 mm·year<sup>-1</sup>, followed by those of Raohe (1010.0 mm·year<sup>-1</sup>), Xiushui (938.4 mm·year<sup>-1</sup>), Ganjiang (844.0 mm·year<sup>-1</sup>) and Fuhe (778.9 mm·year<sup>-1</sup>), respectively. No sufficient differences in other climate variables can be found among the sub-basins in PYLB.

**Table 3.** Basic characteristics of the PYLB.  $\bar{P}$ ,  $\bar{E}_0$ ,  $\bar{R}$ ,  $\bar{T}$ ,  $\bar{U}$ ,  $\bar{RH}$  and  $\bar{R}_n$  represent the mean annual values of precipitation, evaporation, runoff depth, temperature, wind speed, relative humidity and net radiation.

Basin	$\bar{P}$ (mm·Year <sup>-1</sup> )	$\bar{E}_0$ (mm·Year <sup>-1</sup> )	$\bar{R}$ (mm·Year <sup>-1</sup> )	$\bar{T}$ (°C)	$\bar{U}$ (m·s <sup>-1</sup> )	$\bar{RH}$ (%)	$\bar{R}_n$ (MJ·m <sup>-2</sup> ·Year <sup>-1</sup> )
Xiushui	1575.7	937.8	938.4	16.5	1.5	78.4	3101.4
Xinjiang	1810.2	1021.2	1151.8	18.1	2.1	76.8	3172.0
Fuhe	1670.8	1015.3	778.9	18.2	2.7	79.4	3197.4
Ganjiang	1558.7	1015.2	844.0	18.5	1.8	77.9	3214.9
Raohe	1729.6	1001.3	1010.0	17.6	2.0	77.1	3171.0
Whole basin	1639.7	1001.6	894.4	17.9	2.0	77.9	3184.9

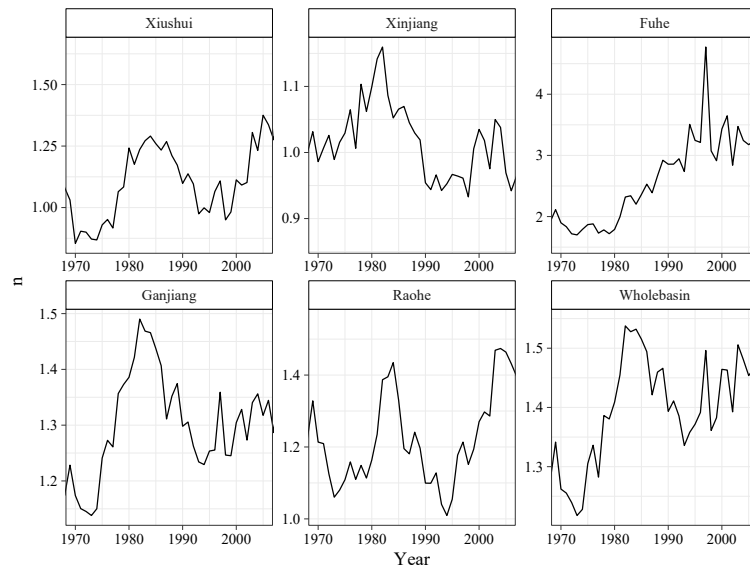
Figure 2 presents the trends of the annual climatic and hydrologic variable series. The change rate is defined as the ratio of the trend slope to the mean annual value. Generally, the PYLB had been warming during the study period, with annual temperature significantly increasing at a rate of 1.44% (i.e., 0.19 °C) per decade. In addition, basin-wide wind speed ( $U$ ) and net radiation ( $R_n$ ) had been declining at 0.17 m/s and 46.30 MJ/m<sup>2</sup> per decade. No significant trend was detected in precipitation and relative humidity (except for Raohe sub-basin). Besides the trend of climatic variables, the runoff trend in the PYLB, as well as the five sub-basins was also calculated, and its results are presented in Figure 2. As presented in Figure 2, no significant trend can be detected in runoff across the PYLB over the whole study period due to its huge inter-annual fluctuations.



**Figure 2.** Changes in climatic variables and runoff in the PYLB.  $R$ ,  $RH$ ,  $U$ ,  $T$ ,  $R_n$  and  $P$  represent runoff, relative humidity, wind speed, temperature, net radiation and precipitation, respectively. The shade of the cell color represents the change rate per decade. The cell labeled with two asterisks (\*\*) denotes the statistically-significant trend at the 1% significance level. The cell without asterisks denotes that the trend is not statistically significant at both the 1% and 5% significance levels.

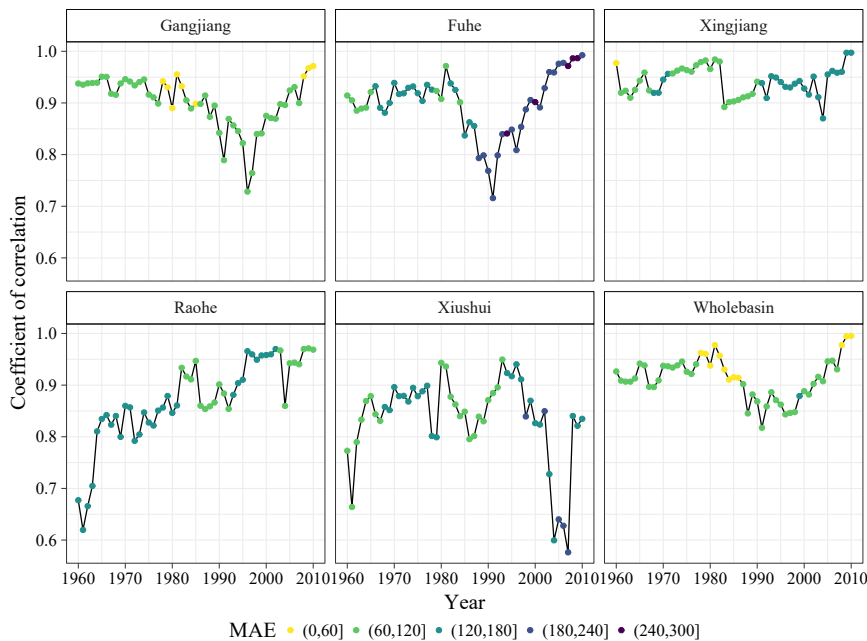
#### 4.2. Temporal and Spatial Pattern of the Catchment Properties' Parameter

Figure 3 shows the temporal variation of the catchment properties' parameters for each sub-basin, as well as the whole PYLB. As shown in Figure 3, on a 10-year moving window scale, the ranges of the  $n$  value are 0.85–1.65, 0.86–1.16, 1.56–4.77, 1.13–1.49 and 1.01–1.56 for Xiushui, Xinjiang, Fuhe, Ganjiang and Raohe sub-basin, respectively. The basin-wide  $n$  value is between 1.22 and 1.55. In sub-basins except for Fuhe, the  $n$  values increased during 1970–1980, followed by a sharp decrease in period from 1980 to 1990 and ended with a slight upward trend in the 2000s. However in Fuhe sub-basin, the  $n$  value kept increasing for the period from 1960 to the 2000s, which almost persists for the whole study period.



**Figure 3.** Temporal variation of the catchment properties' parameter  $n$  for PYLB and each sub-basin during the period from 1960 to 2010. The annual value of  $n$  was calibrated by adapting the Budyko framework with a 10-year moving average, including the five antecedent and precedent years.

In order to evaluate the results of the  $n$  calibration, the correlation coefficient and the mean absolute error (MAE) between the simulated and observed runoff within each 10-year moving window were further calculated and summarized in Figure 4. As shown in Figure 4, despite of the great fluctuations, most of the correlation coefficient values are greater than 0.7 with small mean absolute error (MAE), indicating that the simulated results are acceptable.



**Figure 4.** Correlation between observed and estimated annual runoff within each moving window for the period 1960–2010. The y-axis value of each dot in the figure denotes the coefficient of correlation between the simulated and observed runoff in a 10-year moving window, and the shade of the dot represents the mean absolute error (MAE) between the observed and the simulated annual runoff in each 10-year moving window.

### 4.3. Climatic Elasticity in PYLB

After estimating the parameter  $n$ , we calculated the climate elasticity based on the annual data for the period from 1960 to 2010. Following the framework developed by Yang and Yang [3], the climate elasticity can be estimated according to the mean annual climatic variables. The mean elasticity results for each sub-basin, as well as the whole PYLB for the entire study period are listed in Table 4. As shown in Table 4, the value of precipitation elasticity ( $\epsilon_P$ ) is much larger than other climatic variable elasticities, indicating that runoff is more sensitive to precipitation than to other climatic variables (i.e., radiation, temperature, wind speed and humidity) across the PYLB. Specifically, a 1%  $P$  increase will result in A 1.67% runoff increase; a 1% increase in  $R_n$  and  $T$  will lead to A 0.50% and A 0.22% decrease in runoff, respectively; a 1%  $T$  increase will induce A 0.22% decrease in runoff; and  $RH$  appears to have little influence on runoff. Despite the climate variables, the catchment properties' parameter also influences runoff; a 1% increase in  $n$  will lead to A 0.27% decrease in runoff. Additionally, the climate elasticities in Fuhe sub-basin ARE relative higher than those in other sub-basins, and no sufficient differences are found among the other four sub-basins.

**Table 4.** Average climate elasticities across PYLB for 1960–2010.  $\epsilon_P$ ,  $\epsilon_{Rn}$ ,  $\epsilon_T$ ,  $\epsilon_U$ ,  $\epsilon_{RH}$  and  $\epsilon_n$  represent precipitation elasticity, net radiation elasticity, temperature elasticity, wind speed elasticity, relative humidity elasticity and catchment properties' parameter elasticity, respectively.

Basin	$\epsilon_P$	$\epsilon_{Rn}$	$\epsilon_T$	$\epsilon_U$	$\epsilon_{RH}$	$\epsilon_n$
Xiushui	1.51	−0.40	−0.16	0.05	0.0009	−0.30
Xinjiang	1.44	−0.32	−0.14	0.05	0.0010	−0.27
Fuhe	2.04	−0.74	−0.34	0.14	0.0029	−0.15
Ganjiang	1.65	−0.50	−0.21	0.07	0.0013	−0.32
Raohe	1.57	−0.42	−0.18	0.06	0.0012	−0.26
PYLB	1.67	−0.50	−0.22	0.07	0.0015	−0.27

The temporal variation of runoff elasticities in PYLB is shown in Figure 5. As expected, the climate elasticities across the PYLB keep changing over time. However, the variation shows no monotonic trend except for  $\epsilon_n$  in Fuhe sub-basin. The dominant pattern to emerge from the analysis of runoff elasticities in Figure 5 is that, in the PYLB, the temporal variation of runoff elasticities to climate variables turns out to be a W-shaped curve, which is to say the elasticities decreased in the beginning of the period and then comes in a small period of recovery followed by another decrease and an eventual long-term upward trend. In addition, the temporal pattern of runoff elasticities to the catchment properties' parameter in the PYLB is different; specifically, the catchment properties' parameter elasticity ( $\epsilon_n$ ) values in sub-basins except for Fuhe fluctuate for the period from 1960 to 2000 with a slight downward trend followed by a sharp upward trend in the end of the study period. In contrast, a sharp dip in  $\epsilon_n$  is found for the period from 1960 to 2000 in Fuhe sub-basin and ends with a slight upward trend.

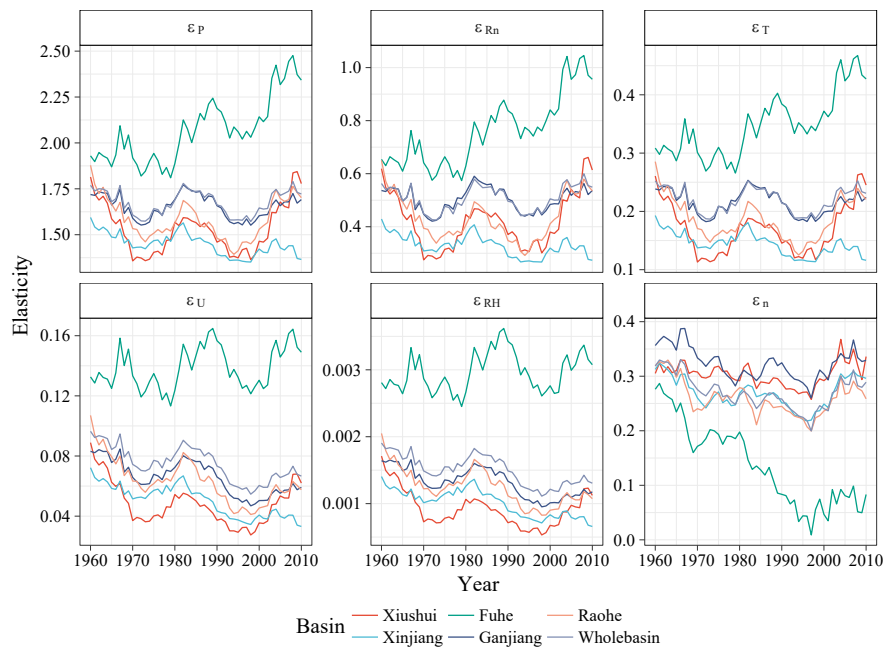


**Figure 5.** Temporal variation of climate elasticities across PYLB during 1960–2010. The annual value of elasticity was calculated by adapting the Budyko framework with a 10-year moving average, including the five antecedent and precedent years.  $\epsilon_P$ ,  $\epsilon_{Rn}$ ,  $\epsilon_T$ ,  $\epsilon_U$ ,  $\epsilon_{RH}$  and  $\epsilon_n$  represent precipitation elasticity, net radiation elasticity, temperature elasticity, wind speed elasticity, relative humidity elasticity and catchment properties’ parameter elasticity, respectively.

#### 4.4. Influence of the Catchment Properties’ Parameter on Climate Elasticities and Runoff Prediction

In Sections 4.2 and 4.3, we evaluated the temporal variation of the catchment properties’ parameter and the derived climate elasticities, and the temporal pattern of the two were similar, which indicates a relationship between  $n$  and climate elasticities. The relationships between  $n$  and derived elasticities are shown in Figure 6. As expected, the catchment properties’ parameter is significantly correlated with the derived elasticities. Specifically, precipitation elasticity, wind speed elasticity and relative humidity elasticity showed significant positive correlations with  $n$ , whereas temperature elasticity and net radiation elasticity were significantly negatively correlated with catchment properties parameter.

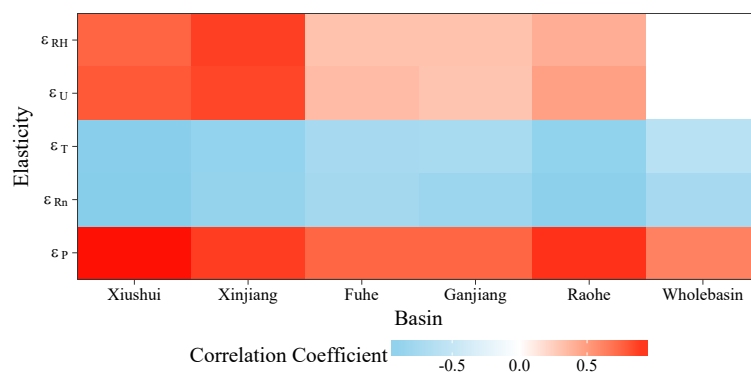


**Figure 6.** Correlation between the calibrated  $n$  and climate elasticities in PYLB, as well as the five sub-basins. Blank denotes no significant correlation between  $n$  and climate elasticities (at the 95% significance level).

Figure 7 shows the differences of two (i.e.,  $dn = 0$  and  $dn$  calculated from the moving window method) predicted runoff trends compared to the observed trend according to Section 4.1. As shown in Figure 7, the predicted runoff trend would get closer to the observed one when taking  $n$  variation into consideration in Xinjiang, Fuhe and the whole PYLB. However, in sub-basins like Xiushui, Ganjiang and Raohe, the prediction error could become larger when  $n$  was considered.

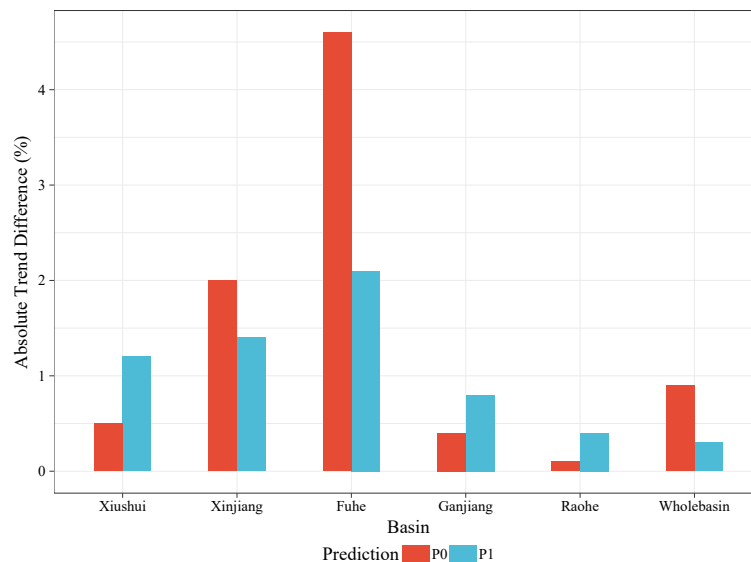


**Figure 7.** Absolute differences between predicted and observed runoff trend. P0 and P1 stand for prediction without consideration of  $n$  and prediction with consideration of  $n$ , respectively.

## 5. Discussion

### 5.1. Potential Factors Influencing the Catchment Properties' Parameter

In this study, with the assumption that the Budyko framework could be applied with moving averages, we estimated the temporal variation of the catchment properties' parameter  $n$  in PYLB, as well as the five sub-basins using a 10-year moving average method. Our results showed that the parameter  $n$  in Equation (7) ranges from 1.0 to 2.0 for most sub-basins in PYLB, consistent with previous findings for the same region [16,51,52]; whereas the  $n$  value in Fuhe sub-basin was notably higher. A comparable result was given in Ye et al. [34], who found that the value of the catchment properties' parameter in Fuhe sub-basin was three times as much as  $n$  values in other sub-basins in PYLB.

Generally, the catchment properties' parameter,  $n$ , alters the partitioning of  $P$  between  $E$  and  $R$  and represents the sum effects of all processes not encapsulated in  $P$  and  $E_p$  [18]. As discussed in previous studies, potential catchment factors influencing the  $n$  value could be classified into four categories: (1) climate intra-annual variability, such as precipitation seasonality, timing intensity and form [53]; (2) catchment geography [17,52], for example slope [17,54], aspect [54] and surface roughness [54]; (3) vegetation characteristics, including vegetation coverage [17,54] vegetation structure [37], effective rooting depth and plant root characteristics [20,29]; (4) edaphic condition, like soil depth [17] and soil moisture or total water storage change (TWSC) [52].

Among the four factors above, vegetation characteristics have always been regarded as the the important factors for  $n$  variation in many previous studies [51,52,55], and it is also the case in the PYLB. Due to the rapid development of urbanization, industrialization and agricultural cultivation [56], PYLB, like many other regions in China, has undergone intensive human activities since 1950, including afforestation and deforestation, land reclamation, river regulation, agriculture intensification and extensive infrastructure construction, which may have exerted considerable impacts on catchment hydrology [34]. Guo et al. [37] applied the SWAT model in PYLB and demonstrated that when

agriculture land changed into forest, accounting for up to 23.3% of the catchment area, it would result in a decrease of annual runoff by up to 3.2%. Figure 8 shows the change of forest coverage and soil erosion area in PYLB for the period from 1960 to 2010 [57]. Remarkably, the forest coverage in PYLB increased dramatically since the 1970s. In addition, other studies also demonstrated that the Normalized Difference Vegetation Index (NDVI) in PYLB presented an increasing trend since the 1980s [35,58,59]. Both historical and remote sensing evidence highlight the increase of vegetation coverage in PYLB, which may play an important role in reducing runoff. The causes of vegetation change include both climate and human factors, such as: (1) the “Grain-for-Green” revegetation project in not only PYLB, but also the entirety of China [60,61]; (2) irrigation and fertilization [59]; and (3) the impact on vegetation due to increasing CO<sub>2</sub> concentration from human activities [62–64].

A previous study [34] also pointed out the importance of soil erosion in the catchment. As shown in Figure 8, an upward trend can be found in the soil erosion area in PYLB during 1960–1990, followed by a dramatic decreasing trend from 1990–2010. Erosion will reduce the water-holding capacity because of rapid water runoff [65], which may increase the amount of runoff in the catchment and, thus, reduce the  $n$  value.

Despite the vegetation coverage and soil erosion area, extensive water utilization is also considered as the main factor that reduces the runoff in PYLB. As demonstrated by Ye et al. [34], the volume of water storage in PYLB increased steadily from 1970 to 2010, especially after the 1990s. The reasons for this are the rapid changes in society and social life, population, economic forces and technological development, which increased the demand and the ability of water supply for industrial and domestic consumptions.

In summary, the increase of  $n$  values in PYLB during the period from 1970 to 1980 could possible be the result of the increased water storage volume due to the rapid development in the catchment; whereas the dramatic increase in soil erosion area in 1980–1990 should enhance the runoff generation in the catchment and could possibly account for the decline in  $n$  for that period. Finally, the upward trend in  $n$  in the 2000s may be the sum effects of decreased erosion area, increased vegetation coverage and water storage volume.

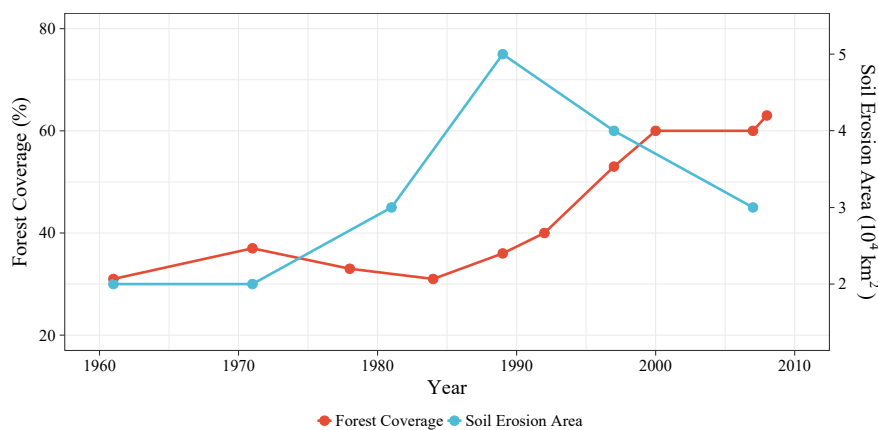


**Figure 8.** Changes of forest coverage and soil erosion area in PYLB from 1960 to 2010.

In addition, the different changing patterns in  $n$  values in Fuhe sub-basin since the 1990s (Figure 3) as compared with other sub-basins may be the result of high water-use efficiency. In Fuhe sub-basin, a previous study [34] suggested that it is the only catchment where the reduction in runoff should be mainly attributed to the intensive human activities. The biggest irrigation farmland, as well as the irrigation systems of Jiangxi province are also located in the middle and lower reach of Fuhe, which will notably increase the water utilization and directly decrease runoff. Hence, in the Fuhe sub-basin, a relatively lower runoff  $Q$ , which means a higher  $E$  (calculated as  $R = P - E$ ) when  $P$  varies little

among all of the sub-basins, results in the higher estimated value of  $n$ . In addition, the intensive human activities may possibly contribute to the increase of  $n$  in Fuhe sub-basin.

### 5.2. Uncertainty and the Limitations of This Study

In the present study, we assumed that the long-term water balance of a catchment will follow the Budyko curve if climate change occurs and further estimated the temporal variation of climate elasticities across the PYLB. Remarkable, as shown in Equation (7), the catchment water balance will follow one Budyko curve only when  $n$  keeps constant. Hence, to evaluate the temporal variation of climate elasticities across the PYLB, we treated parameter  $n$  as a changeable constant, that is the parameter will keep constant in each relatively shorter sub-period (five or 10 years) and will change as sub-periods change. Following the simple assumption, the temporal variation of climate elasticities can be estimated.

However, when applying the  $n$  trend results in runoff prediction, the results were not as expected. There were still considerable differences between calculated and observed trend in runoff. The possible causes are the following: (1) some climatic variables or runoff itself have relatively large variabilities, but no significant trends. (2) under the framework developed by Yang and Yang [3], when calculating the runoff trend, the elasticity itself should keep constant, which is not the case in reality. This highlights a shortcoming in the analyses presented here and of the framework as a whole, which is that values of  $n$  are not easily estimated a priori for a given area. In practical, the values of  $n$  have to be either estimated or, if runoff data exist, fitted to observational data, thus limiting the framework to gauged catchments and to historical conditions. Additionally, the framework used in this study only assesses the changes in steady state conditions. In other words, when the effects of a 10% change in  $P$ , for example, have been discussed, it is assumed that such a change has no bearing on soil storage dynamics.

In addition, other possible influences of data error on the results are yet to be investigated. Meteorological data from 14 weather stations in this study area (PYLB) might not be sufficient coverage for such a larger-scale catchment. The influence of human activities on the estimation of mean annual  $E$  is not considered. Although the calibrated catchment properties' parameter  $n$  in this study well reflects the average catchment condition in most periods, these could still affect the final results to some extent.

Consequently, we should further make  $n$  as a function of climate, vegetation and other potential variables, i.e.,  $n = f(C, V, \dots)$ , which should be able to quantify the temporal variation of  $n$  in a finer time scale (e.g., yearly) and make the  $n$  a priori estimate. By combing this function with the original Budyko hypothesis, the climate impact on runoff should include not only the impacts from  $P$  and  $E_0$  change, but also the impacts from the changes in other climate characteristics (such as climate seasonality and mean storm depth) and vegetation change caused by climate change.

## 6. Conclusions

As an important part of the hydrological cycle, the change of runoff can significantly affect water resources, society's safety and ecosystem health [66]. Understanding the effects of climate and land cover changes on water yield is a challenging component in the assessments of future water resources [53]. In this study, we used the M-C-Y equation [16,26,27], based on the widely-used Budyko framework, to quantify the temporal and spatial differences of climate elasticity of runoff in PYLB. By using the moving average method, we highlighted the influence of the catchment properties' parameter ( $n$ ) variation on the climate elasticity, as well as runoff prediction. From the results obtained in this study, the following conclusions can be made:

1. Changes in climatic variables and runoff were found using the Mann–Kendall test and Sen's slope estimator. Annual temperature in PYLB significantly increased at a rate of 1.44% (i.e., 0.19 °C) per decade. Basin-wide wind speed ( $U$ ) and net radiation ( $R_n$ ) had been declining at 0.17 m/s and 46.30 MJ/m<sup>2</sup> per decade. No significant trend was detected in precipitation and relative humidity.

2. The catchment properties' parameter is not constant during the whole study period. As we evaluated, in sub-basins, except for the Fuhe, a slight upward trend can be found during 1970–1980, followed by a decrease trend in the period from 1980 to 1990. However, the  $n$  value in Fuhe sub-basin kept increasing for the period from 1970 to 2010, which is almost persistent for the whole study period. In addition, the derived climate elasticities were significantly correlated with the catchment properties' parameter, indicating that the catchment properties' parameter was the dominant factor influencing climate elasticity in PYLB in the past 50 years.
3. The moving window method presented in this study is relatively simple, but it is a feasible method to detect the temporal variation of climate elasticity and catchment properties. Taking the variation of the catchment properties' parameter into consideration when predicting future runoff may enhance the accuracy.

**Acknowledgments:** We would like to thank the Editor, Associate Editor and two anonymous reviewers for their constructive comments, which have noticeably improved the final manuscript. The research was supported by National Natural Science Foundation of China (41371121, 41661018), Science and Technology Project of JiangSu Province (BZ2014005 and BE2014739) and National Science & Technology Pillar Program during the Twelfth Five-year Plan Period (2014BAC09B02).

**Author Contributions:** Hongxiang Fan and Ligang Xu conceived and designed the study; Hongxiang Fan and Hui Tao analyzed the data; Wenjuan Feng, Junxiang Cheng and Hailin You contributed data; Hongxiang Fan wrote the paper.

**Conflicts of Interest:** The authors declare no conflicts of interest.

## References

1. Intergovernmental Panel on Climate Change. *Climate Change*; Intergovernmental Panel on Climate Change: Geneva, Switzerland, 2001.
2. Solomon, S. *Climate Change 2007—The Physical Science Basis: Working Group I Contribution to the Fourth Assessment Report of the IPCC*; Cambridge University Press: Cambridge, UK, 2007; Volume 4,
3. Yang, H.B.; Yang, D.W. Derivation of climate elasticity of runoff to assess the effects of climate change on annual runoff. *Water Resour. Res.* **2011**, *47*, doi:10.1029/2010WR009287.
4. Donohue, R.J.; Roderick, M.L.; McVicar, T.R. Assessing the differences in sensitivities of runoff to changes in climatic conditions across a large basin. *J. Hydrol.* **2011**, *406*, 234–244.
5. Milly, P.C.D.; Dunne, K.A. Macroscale water fluxes—2. Water and energy supply control of their interannual variability. *Water Resour. Res.* **2002**, *38*, doi:10.1029/2001WR000760.
6. Sankarasubramanian, A.; Vogel, R.M.; Limbrunner, J.F. Climate elasticity of streamflow in the United States. *Water Resour. Res.* **2001**, *37*, 1771–1781.
7. Kundzewicz, Z.W.; Stakhiv, E.Z. Are climate models “ready for prime time” in water resources management applications, or is more research needed? *Hydrol. Sci. J.* **2010**, *55*, 1085–1089.
8. Fu, B. On the calculation of the evaporation from land surface. *Sci. Atmos. Sin.* **1981**, *5*, 23–31.
9. Dooge, J.; Bruen, M.; Parmentier, B. A simple model for estimating the sensitivity of runoff to long-term changes in precipitation without a change in vegetation. *Adv. Water Resour.* **1999**, *23*, 153–163.
10. Nash, L.L.; Gleick, P.H. Sensitivity of streamflow in the Colorado basin to climatic changes. *J. Hydrol.* **1991**, *125*, 221–241.
11. Revelle, R.R.; Waggoner, P.E. Effects of a Carbon Dioxide-Induced Climatic Change on Water Supplies in 7 the Western United States. *Month* **1983**, *419*, 432.
12. Schaake, J.C.; Waggoner, P. From climate to flow. In *Climate Change and US Water Resources*; John Wiley & Sons: Hoboken, NJ, USA, 1990; pp. 177–206.
13. Vogel, R.M.; Wilson, I.; Daly, C. Regional regression models of annual streamflow for the United States. *J. Irrig. Drain. Eng.* **1999**, *125*, 148–157.
14. Milly, P.; Betancourt, J.; Falkenmark, M.; Hirsch, R.; Kundzewicz, Z.; Lettenmaier, D.; Stouffer, R. Climate change. Stationarity is dead: whither water management? *Science* **2008**, *319*, 573–574.
15. Budyko, M. *Climate and Life*, 508 pp; Academic Press: San Diego, CA, USA, 1974; pp. 72–191.
16. Yang, H.; Yang, D.; Lei, Z.; Sun, F. New analytical derivation of the mean annual water-energy balance equation. *Water Resour. Res.* **2008**, *44*, doi:10.1029/2007WR006135.

17. Trancoso, R.; Larsen, J.R.; Mcalpine, C.; Mcvicar, T.R.; Phinn, S. Linking the Budyko framework and the Dunne diagram. *J. Hydrol.* **2016**, *535*, 581–597.
18. Roderick, M.L.; Farquhar, G.D. A simple framework for relating variations in runoff to variations in climatic conditions and catchment properties. *Water Resour. Res.* **2011**, *47*, doi:10.1029/2010WR009826.
19. Yang, D.; Shao, W.; Yeh, P.J.F.; Yang, H.; Kanae, S.; Oki, T. Impact of vegetation coverage on regional water balance in the nonhumid regions of China. *Water Resour. Res.* **2009**, *45*, 450–455.
20. Cong, Z.; Zhang, X.; Li, D.; Yang, H.; Yang, D. Understanding Hydrological Trends by Combining the Budyko Hypothesis and a Stochastic Soil Moisture Model. *Hydrol. Sci. J.* **2014**, *60*, 145–155.
21. Yang, D.; Sun, F.; Liu, Z.; Cong, Z.; Lei, Z. Interpreting the complementary relationship in non-humid environments based on the Budyko and Penman hypotheses. *Geophys. Res. Lett.* **2006**, *33*, 122–140.
22. Yang, D.; Sun, F.; Liu, Z.; Cong, Z.; Ni, G.; Lei, Z. Analyzing spatial and temporal variability of annual water-energy balance in nonhumid regions of China using the Budyko hypothesis. *Water Resour. Res.* **2007**, *43*, 436–451.
23. Zheng, H.; Lu, Z.; Zhu, R.; Liu, C.; Sato, Y.; Fukushima, Y. Responses of streamflow to climate and land surface change in the headwaters of the Yellow River Basin. *Water Resour. Res.* **2009**, *45*, 641–648.
24. Arora, V.K. The use of the aridity index to assess climate change effect on annual runoff. *J. Hydrol.* **2002**, *265*, 164–177.
25. Gong, L.B.; Xu, C.Y.; Chen, D.L.; Halldin, S.; Chen, Y.Q.D. Sensitivity of the Penman-Monteith reference evapotranspiration to key climatic variables in the Changjiang (Yangtze River) basin. *J. Hydrol.* **2006**, *329*, 620–629.
26. Choudhury, B. Evaluation of an empirical equation for annual evaporation using field observations and results from a biophysical model. *J. Hydrol.* **1999**, *216*, 99–110.
27. Mezentsev, V. More on the calculation of average total evaporation. *Meteorol. Gidrol.* **1955**, *5*, 24–26.
28. Penman, H.L. Natural evaporation from open water, bare soil and grass. *Proc. R. Soc. Lond. Ser. A Math. Phys. Sci.* **1948**, *9*, 120–145.
29. Donohue, R.J.; Roderick, M.L.; Mcvicar, T.R. Roots, storms and soil pores: Incorporating key ecohydrological processes into Budyko's hydrological model. *J. Hydrol.* **2012**, *436–437*, 35–50.
30. CSIRO. *Water Availability in the Murray-Darling Basin. A Report to the Australian Government from the CSIRO Murray-Darling Basin Sustainable Yields Project*; Csiro Australia: Kawana, Australia, 2008.
31. Donohue, R.J.; Mcvicar, T.R.; Roderick, M.L. Assessing the ability of potential evaporation formulations to capture the dynamics in evaporative demand within a changing climate. *J. Hydrol.* **2010**, *386*, 186–197.
32. Lei, S.; Zhang, X.P.; Li, R.F.; Xu, X.H.; Fu, Q. Analysis the changes of annual for Poyang Lake wetland vegetation based on MODIS monitoring. *Procedia Environ. Sci.* **2011**, *10 Pt B*, 1841–1846.
33. Shankman, D.; Liang, Q. Landscape Changes and Increasing Flood Frequency in China's Poyang Lake Region. *Prof. Geogr.* **2003**, *55*, 434–445.
34. Ye, X.C.; Zhang, Q.; Liu, J.; Li, X.H.; Xu, C.Y. Distinguishing the relative impacts of climate change and human activities on variation of streamflow in the Poyang Lake catchment, China. *J. Hydrol.* **2013**, *494*, 83–95.
35. Tan, Z.; Tao, H.; Jiang, J.; Zhang, Q. Influences of Climate Extremes on NDVI (Normalized Difference Vegetation Index) in the Poyang Lake Basin, China. *Wetlands* **2015**, *35*, 1033–1042.
36. Xu, L.G.; Zhu, M.L.; He, B.; Wang, X.L.; Zhang, Q.; Jiang, J.H.; Razafindrabe, B.H.N. Analysis of Water Balance in Poyang Lake Basin and Subsequent Response to Climate Change. *J. Coast. Res.* **2014**, *68*, 136–143.
37. Guo, H.; Hu, Q.; Jiang, T. Annual and seasonal streamflow responses to climate and land-cover changes in the Poyang Lake basin, China. *J. Hydrol.* **2008**, *355*, 106–122.
38. Dai, X.; Wan, R.; Yang, G. Non-stationary water-level fluctuation in China's Poyang Lake and its interactions with Yangtze River. *J. Geogr. Sci.* **2015**, *25*, 274–288.
39. Zhu, H.; Zhang, B. Poyang Lake—Hydrology. In *Biology. Deposition. Wetland. Exploitation and Rebuilding*; University of Science and Technology of China Press: Hefei, China, 1997; pp. 146–233.
40. Allen, R.G.; Pereira, L.S.; Raes, D.; Smith, M. *Crop Evapotranspiration—Guidelines for Computing Crop Water Requirements—FAO Irrigation and Drainage Paper 56*; Food and Agriculture Organization of the United Nations: Rome, Italy, 1998; Volume 300, p. D05109.
41. Zhang, L.L.; Yin, J.X.; Jiang, Y.Z.; Wang, H. Relationship between the hydrological conditions and the distribution of vegetation communities within the Poyang Lake National Nature Reserve, China. *Ecol. Inform.* **2012**, *11*, 65–75.

42. Zhang, Q.; Li, L.; Wang, Y.G.; Werner, A.D.; Xin, P.; Jiang, T.; Barry, D.A. Has the Three-Gorges Dam made the Poyang Lake wetlands wetter and drier? *Geophys. Res. Lett.* **2012**, *39*, doi:10.1029/2012GL053431.
43. Thiessen, A.H. Precipitation averages for large areas. *Mon. Weather Rev.* **1911**, *39*, 1082–1089.
44. Mann, H.B. Nonparametric Tests Against Trend. *Econometrica* **1945**, *13*, 245–259.
45. Sen, Z. Probabilistic formulation of spatio-temporal drought pattern. *Theor. Appl. Climatol.* **1998**, *61*, 197–206.
46. Rousseeuw, P.J.; Leroy, A.M. *Robust Regression and Outlier Detection*; Wiley-Interscience: Hoboken, NJ, USA, 1987; pp. 260–261.
47. Bagrov, N. Mean long-term evaporation from land surface. *Meteorol. Gidrol.* **1953**, *10*, 21–30.
48. Soetaert, K.; Herman, P.M.J. (Eds.) *A Practical Guide to Ecological Modelling: Using R as a Simulation Platform*; Springer: Berlin/Heidelberg, Germany, 2009.
49. Schaake, J.; Liu, C. Development and application of simple water balance models to understand the relationship between climate and water resources. In Proceedings of the Baltimore Symposium—New Directions for Surface Water Modeling, Baltimore, MD, USA, 15–17 May 1989.
50. R Development Core Team. *R: A Language and Environment for Statistical Computing*; R Foundation for Statistical Computing: Vienna, Austria, 2016.
51. Yang, H.; Qi, J.; Xu, X.; Yang, D.; Lv, H. The regional variation in climate elasticity and climate contribution to runoff across China. *J. Hydrol.* **2014**, *517*, 607–616.
52. Zhang, D.; Liu, X.; Zhang, Q.; Liang, K.; Liu, C. Investigation of factors affecting intra-annual variability of evapotranspiration and streamflow under different climate conditions. *J. Hydrol.* **2016**, *543*, 759–769.
53. Berghuijs, W.R.; Woods, R.A. Correspondence: Space-time asymmetry undermines water yield assessment. *Nat. Commun.* **2016**, *7*, 11603.
54. Liu, M.; Xu, X.; Wang, D.; Sun, A.Y.; Wang, K. Karst catchments exhibited higher degradation stress from climate change than the non-karst catchments in southwest China: An ecohydrological perspective. *J. Hydrol.* **2016**, *535*, 173–180.
55. Li, D.; Pan, M.; Cong, Z.; Zhang, L.; Wood, E. Vegetation control on water and energy balance within the Budyko framework. *Water Resour. Res.* **2013**, *49*, doi:10.1002/wrcr.20107.
56. Wang, X.L.; Han, J.Y.; Xu, L.G.; Wan, R.R.; Chen, Y.W. Soil Characteristics in Relation to Vegetation Communities in the Wetlands of Poyang Lake, China. *Wetlands* **2014**, *34*, 829–839.
57. China Statistics Press. *Jiangxi Statistical Yearbook*; China Statistics Press: Beijing, China, 2016. (In Chinese)
58. Zhu, F.F.; Cheng, Q.Z. Spatial-temporal changes of NDVI and their relations with climate factors in Poyang Lake valley. *Acta Agric. Jiangxi* **2012**, *24*, 98–102.
59. Piao, S.; Fang, J.; Zhou, L.; Guo, Q.; Henderson, M.; Ji, W.; Li, Y.; Tao, S. Interannual variations of monthly and seasonal normalized difference vegetation index (NDVI) in China from 1982 to 1999. *J. Geophys. Res. Atmos.* **2003**, *108*, doi:10.1029/2002JD002848.
60. Mcvicar, T.R.; Li, L.T.; van Niel, T.G.; Zhang, L.; Li, R.; Yang, Q.K.; Zhang, X.P.; Mu, X.M.; Wen, Z.M.; Liu, W.Z. Developing a decision support tool for China's re-vegetation program: Simulating regional impacts of afforestation on average annual streamflow in the Loess Plateau. *For. Ecol. Manag.* **2007**, *251*, 65–81.
61. Liu, Q.; Mcvicar, T.R. Assessing climate change induced modification of Penman potential evaporation and runoff sensitivity in a large water-limited basin. *J. Hydrol.* **2012**, *464–465*, 352–362.
62. Donohue, R.J.; Roderick, M.L.; Mcvicar, T.R.; Farquhar, G.D. Impact of CO<sub>2</sub> fertilization on maximum foliage cover across the globe's warm, arid environments. *Geophys. Res. Lett.* **2013**, *40*, 3031–3035.
63. Bond, W.J.; Midgley, G.F. Carbon dioxide and the uneasy interactions of trees and savannah grasses. *Philos. Trans. R. Soc. Lond.* **2012**, *367*, 601–612.
64. Iversen, C.M. Digging deeper: fine-root responses to rising atmospheric CO<sub>2</sub> concentration in forested ecosystems. *New Phytol.* **2010**, *186*, 346–357.
65. Zuazo, V.H.D. Soil-erosion and runoff prevention by plant covers. A review. *Agron. Sustain. Dev.* **2008**, *28*, 65–86.
66. Sun, S.L.; Chen, H.S.; Ju, W.M.; Song, J.; Zhang, H.; Sun, J.; Fang, Y.J. Effects of climate change on annual streamflow using climate elasticity in Poyang Lake Basin, China. *Theor. Appl. Climatol.* **2013**, *112*, 169–183.

